6-28-2019

Cobalt Superoxo and Alkylperoxo Complexes Derived from Reaction of Ring-Cleaving Dioxygenase Models with O_2

Praveen Kumar
Marquette University

Sergey V. Lindeman
Marquette University, sergey.lindeman@marquette.edu

Adam T. Fiedler
Marquette University, adam.fiedler@marquette.edu

Journal of the American Chemical Society, Vol. 114, No. 28 (June 28, 2019): 10984-10987. DOI.

Cobalt Superoxo and Alkylperoxo Complexes Derived from Reaction of Ring-Cleaving Dioxygenase Models with O_2

Praveen Kumar
Department of Chemistry, Marquette University, Milwaukee, Wisconsin
Sergey V. Lindeman
Department of Chemistry, Marquette University, Milwaukee, Wisconsin
Adam T. Fiedler
Department of Chemistry, Marquette University, Milwaukee, Wisconsin

Abstract

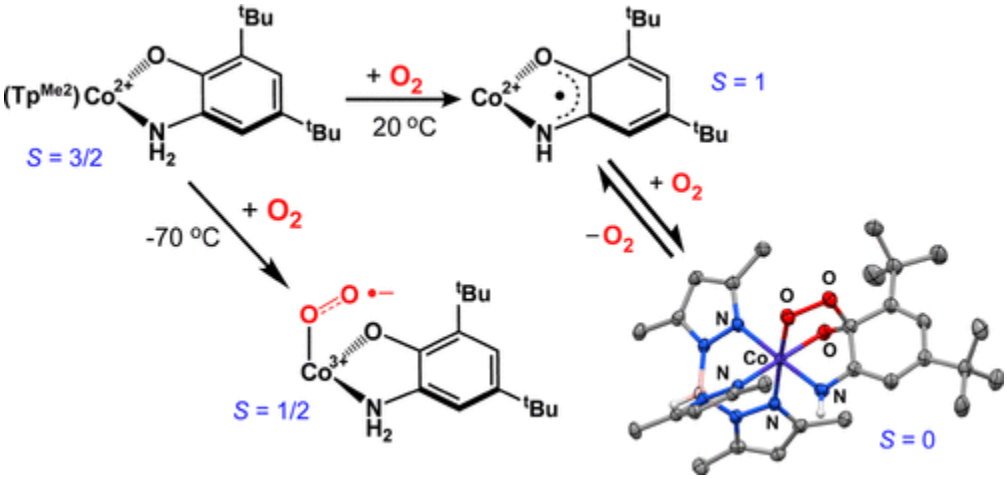

The syntheses and O_2 reactivities of active-site models of cobalt-substituted ring-cleaving dioxygenases are presented. The pentacoordinate cobalt(II)-aminophenolate complex, [Co(Tp^{Me2})(^{tBu2}APH)], gives rise to two distinct dioxygen adducts at reduced temperatures. The first is a paramagnetic (S = 1/2) cobalt(III)-superoxo species that was characterized with spectroscopic and computational techniques. The identity of the second Co/O_2 adduct was elucidated by X-ray crystallography, which revealed an unprecedented cobalt(III)-alkylperoxo structure generated by O_2 addition to the metal ion and ligand. These results provide synthetic precedents for proposed intermediates in the catalytic cycles of O_2-activating cobalt enzymes.

The bacterial breakdown of organic compounds, including human-generated pollutants, often requires dioxygenase enzymes that oxidatively cleave aromatic carbon–carbon bonds using O_2.(1) Substrates of these ring-cleaving dioxygenases include substituted catechols, *o*-aminophenols, 1,4-hydroquinones, and salicylates.(2) The active sites of most ring-cleaving dioxygenases feature a mononuclear nonheme iron center bound facially to one Glu (or Asp) and two His residues.(3) However, recent studies revealed that an extradiol catechol dioxygenase (CatD), homoprotocatechuate-2,3-dioxygenase (HPCD), exhibits equal or greater activity with Mn or Co in the active site.(4) The “promiscuity” of HPCD supports the mechanistic proposal that O_2 activation by ring-cleaving dioxygenases does not necessitate a change in metal oxidation state. Instead, the metal facilitates the transfer of one electron from the coordinated substrate to O_2, thereby yielding a M(II)-superoxo species with an (imino)semiquinone radical (**B** in Scheme 1).(5) Formation of a substrate-based radical encourages attack by the superoxide ligand to generate a putative alkylperoxo species (**C**), which undergoes rearrangement to insert an O atom into the substrate ring (**D**).(6) Analogous mechanisms are likely employed by *o*-aminophenol and 1,4-hydroquinone dioxygenases.(7)

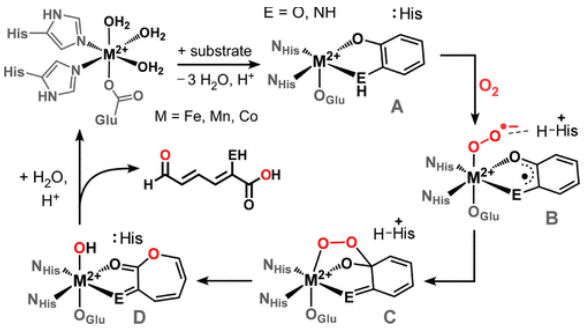

Scheme 1. Proposed Mechanism of Ring-Cleaving Dioxygenases

The surprising activity of metal-substituted HPCD has stimulated the synthesis of extradiol CatD models featuring Co and Mn. Yet complexes that replicate the monoanionic, bidentate coordination of the catecholate ligand in the enzyme active site are still lacking. Recently, the Riordan and Hikichi groups reported Co and Mn complexes, respectively, that feature a monoanionic catecholate ligand bound in a monodentate manner.(8,9) Exposure of these complexes to O_2 results in formation of the corresponding M(II)-semiquinonate (SQ) species via loss of an electron and proton (i.e., net H atom transfer, HAT). Thus, the CatD models fail to replicate the initial O_2 binding step of the enzymatic mechanism. In some cases, further reaction of the Co(II)-SQ complexes with O_2 affords the intradiol ring-cleavage products in low yield.(8)

To avoid the shortcomings of the cobalt-catecholate complexes, we decided to pursue cobalt(II) dioxygenase models that contain an aminophenolate ligand instead. Aminophenol dioxygenases (APDOs) are closely related to extradiol CatDs both structurally and mechanistically,(2) and although a cobalt-substituted APDO has not been generated to date, it is reasonable to expect such an enzyme to display activity. More importantly, we reckoned that the less acidic $-NH_2$ donor would deter formation of a Co(II)-iminosemiquinone (ISQ) species and provide access to biologically relevant O_2 reaction pathways. This hypothesis proved correct, and herein we describe the synthesis of two mononuclear Co(II) complexes (**1** and **2** in Figure 1) that feature a monoanionic, bidentate aminophenolate ligand. The 2-histidine-1-carboxylate facial triad of the enzymatic active site is modeled with the Tp^{R2} ligand (R = Ph (**1**) or Me (**2**); Tp^{R2} = hydrotris(pyrazolyl-1-yl)borate substituted with R-groups at the 3- and 5-positions). Although HAT reactivity is observed for **1** and **2** under certain conditions, the latter complex gives rise to O_2-derived intermediates not observed for the analogous catecholate complexes, including a cobalt-superoxo species that resembles intermediate **B**. Furthermore, we report the first X-ray structure of a cobalt-alkylperoxo complex with a structure akin to **C** in the proposed ring-cleaving mechanism.

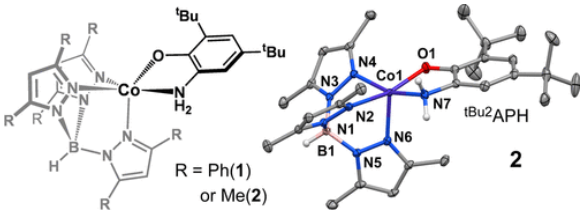

Figure 1. Left: Schematic drawing of [Co(Tp^{R2})(^{tBu2}APH)] (**1** and **2**). Right: X-ray crystal structure of **2**.

The crystal structures of complexes **1** and **2** each revealed a five-coordinate Co(II) center in which the monoanionic ^{tBu2}APH ligand binds in a bidentate fashion (Figure 1). The Tp^{R2} ligands coordinate facially with average Co–N_{Tp} bond distances of 2.11 Å. The Co–N/O bond distances (Table S1) are characteristic of pentacoordinate, high-spin Co(II) complexes. X-band EPR spectra of **1** and **2** (Figure S3) exhibit features arising from the $m_s = \pm 3/2$ doublet of the $S = 3/2$ manifold ($D < 0$). In both spectra, hyperfine splitting from the ^{59}Co nucleus is evident in the low-field resonance near $g \sim 7$ (A_{Co} = 85 G for **2**).

Complex **1** reacts slowly with O_2 to yield a stable, dark green species (**1^{ox}**; Figure 2a). X-ray crystallography determined that **1^{ox}**, like its precursor, is a neutral five-coordinate complex. The Co–N_{Tp} bond distances change only slightly from **1** to **1^{ox}** (Table S1), suggesting that the Co center remains divalent and high-spin. Despite these similarities, comparison of the two structures reveals that the ^{tBu2}APH ligand of **1** has been oxidized to an ISQ radical in **1^{ox}**. The change is apparent in the shorter O1–C1 and N2–C2 bond distances of **1^{ox}**, as well as the quinoidal distortion of its C–C bonds (Figure 2b). Using the "metrical oxidation state" method developed by Brown,(10) the ^{tBu2}ISQ ligand of **1^{ox}** carries a charge of −0.95, near the ideal value of −1.0 for an ISQ ligand. The presence of an ^{tBu2}ISQ radical is also evident from characteristic $\pi \rightarrow \pi^*$ features in the 600–800 nm region of the absorption spectrum that overlap with Co(II) d-d bands (Figure 2a).(11) Complex **1^{ox}** is EPR-silent and the

observed magnetic moment of 2.9 μ_B (S = 1) is indicative of antiferromagnetic coupling between the Co(II) and ^{tBu2}ISQ spins.

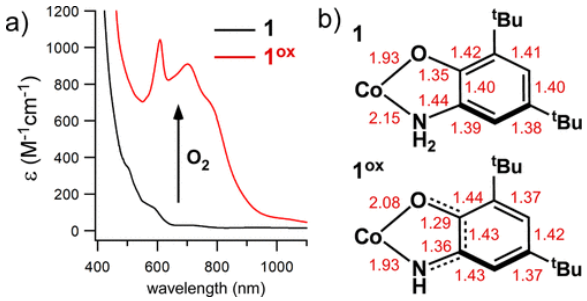

Figure 2. (a) UV–vis absorption spectra of **1** and **1^{ox}** in CH_2Cl_2 at 20 °C. (b) Selected bond distances (Å) for the ^{tBu2}APH and ^{tBu2}ISQ ligands in X-ray structures of **1** and **1^{ox}**, respectively.

Likewise, exposure of **2** to O_2 at room temperature (RT) yields a green species (**2^{ox}**) with spectral and magnetic properties similar to **1^{ox}** (Figure S4). A notable difference, however, is that **2^{ox}** decays within minutes at 20 °C, which hindered the growth of suitable crystals. Significantly, **2^{ox}** can also be generated under anaerobic conditions by treating **2** with one equivalent of 2,4,6-tri-*tert*-butylphenoxy radical (TTBP$^{\bullet}$), a well-known H atom abstractor (Figure S4). This result demonstrates that the conversion of **2** → **2^{ox}** involves loss of a proton and electron to generate [$Co^{II}(Tp^{Me2})(^{tBu2}ISQ)$]. Nuclear magnetic resonance (NMR) analysis of the reaction mixture after decay of **2^{ox}** in air found that 3,5-di-*tert*-butyl-*o*-benzoquinone (DTBQ) is the only product derived from the ^{tBu2}APH ligand (Figure S5). Thus, the overall O_2 reaction does not result in oxygenated or ring-cleaved products; instead, the ^{tBu2}APH ligand undergoes two-electron oxidation to the corresponding *o*-iminobenzoquinone, followed by hydrolysis to DTBQ upon aqueous workup.

While the O_2 reactivity of **1** and **2** at RT is dominated by HAT chemistry, we found that it is possible to observe novel Co/O_2 adducts at reduced temperatures. Reaction of **2** with O_2 at −78 °C in CH_2Cl_2 or THF generates a metastable pink species (**2-O$_2$**) with absorption features at λ_{max} = 505 and 800 nm (Figure 3a). Purging the solution with Ar does not regenerate **2**, and warming causes **2-O$_2$** to convert to **2^{ox}**. The X-band EPR spectrum of **2-O$_2$** presents a S = 1/2 signal with g-values of 2.084, 2.007, 1.957 and ^{59}Co hyperfine splitting of 28 G (Figure 3b). Quantification of the EPR signal indicates that **2-O$_2$** accounts for ~80% of the Co in the sample, with the remainder being starting complex. Both the UV–vis and EPR spectra of **2-O$_2$** are strikingly similar to those previously reported for Co/O_2 adducts.(12) In particular, the clustering of the g-values near 2.0 and the small A_{Co}-value of **2-O$_2$** (relative to its Co(II) precursor) are distinctive characteristics of cobalt(III)-superoxo species, reflecting localization of the unpaired electron on the superoxo ligand. The presence of a superoxo-to-Co(III) charge transfer (CT) transition near 500 nm, as observed for **2-O$_2$**, is also a common feature of known cobalt(III)-superoxo complexes in noncorrinoid environments.(12) Interestingly, complex **1** is unreactive with O_2 at low temperatures, suggesting that sterics modulate the energetics of O_2 binding.

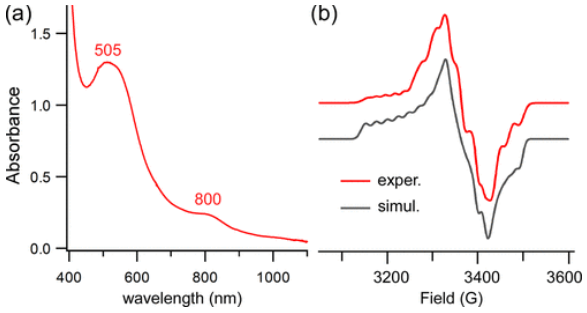

Figure 3. (a) UV–vis absorption spectrum of **2-O$_2$** obtained by reaction of **2** with O_2 in THF at −70 °C. [**2**]$_{initial}$ = 1.25 mM. (b) X-band EPR spectrum (red) of **2-O$_2$** in frozen THF at 77 K. Parameters for the simulated spectrum (gray) are provided in the SI.

The geometric and electronic structures of **2-O_2** were further analyzed using density functional theory (DFT) calculations. The geometry-optimized structure (Figure S6) features an end-on superoxo ligand in a bent conformation. The superoxo nature of the O_2 ligand is reflected in the computed O–O distance of 1.278 Å. The six-coordinate Co(III) center is low-spin and nearly all of the unpaired spin density resides on the superoxo ligand, consistent with the EPR data. The computed ^{59}Co **A**-tensor is anisotropic with a dominant hyperfine splitting of 26 G, in excellent agreement with the experimental value. The *g*-values predicted by CASSCF/NEVPT2 calculations ($g_{1,2,3}$ = 2.060, 1.991 and 1.979) reproduce the weak anisotropy of the **2-O_2** signal. Thus, the computational data further corroborate the assignment of **2-O_2** as a cobalt(III)-superoxo species.

Interestingly, we found that a second Co/O_2 adduct with spectroscopic features distinct from **2-O_2** is generated when **2^{ox}** is treated with O_2 at reduced temperatures. Aerobic solutions of **2^{ox}** in CH_3CN and CH_2Cl_2 change from dark green to light brown upon cooling. Monitoring the process by UV–vis spectroscopy revealed that the species generated at low temperature (**3**) lacks well-defined absorption features in the visible region (Figure 4a). The absorption features of **2^{ox}** return when the solution is warmed to RT, but full intensity is not recovered due to its instability. No color change is observed during cooling if **2^{ox}** is generated anaerobically via reaction with TTBP$^{\bullet}$, indicating that formation of **3** requires O_2. The characteristics of the **2^{ox}** → **3** conversion are reminiscent of those previously reported for the O_2 reaction of cobalt(II)-semiquinonate complexes at reduced temperatures.(8b,9b) Because of this, we prepared and structurally characterized [Co^{II}(Tp^{Me2})(^{tBu2}SQ)] (**4**; Figure S7), the SQ analogue of **2^{ox}**. Complex **4** reacts with O_2 at T < −40 °C to give a brown chromophore (**5**) with absorption features similar to those of **3** (Figure S8). Like **3**, species **5** is EPR-silent and variable-temperature NMR experiments indicate that both Co/O_2 adducts are diamagnetic (Figures S9–S11).

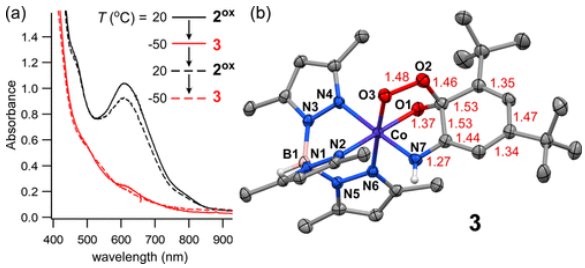

Figure 4. (a) UV–vis spectral changes for the thermal interconversion of **2^{ox}** (black) and **3** (red) in CH_2Cl_2 in the presence of O_2. [Co] = 0.7 mM (b) Ellipsoid plot derived from the X-ray structure of **3**. Selected bond lengths (Å) are provided in red.

Due to its stability at temperatures below −25 °C, we succeeded in growing light brown crystals of **3** for X-ray analysis. The resulting crystal structure revealed a neutral cobalt-alkylperoxo complex in which the O_2-derived atoms form a bridge between Co and C1 of the ligand (Figure 4b), thereby generating a five-membered metallocycle. The O2–O3 distance of 1.482(3) Å is typical of alkylperoxo ligands, and the sp^3 hybridization of the C1-atom is evident from its average bond angle of 110° ± 7°. The Co–N/O bond distances in **3** are shorter than those of **2** by an average of 0.15 Å, indicating a change from high-spin Co(II) to low-spin Co(III). Comparison of **3** to **1^{ox}** reveals that the quinoidal distortion of the ligand is far more pronounced in the former complex, and the metric parameters observed for **3** are characteristic of iminobenzoquinone ligands.(10) Thus, formation of **3** is a two-electron process involving oxidation of both the Co center and ^{tBu2}ISQ ligand (Scheme 2).

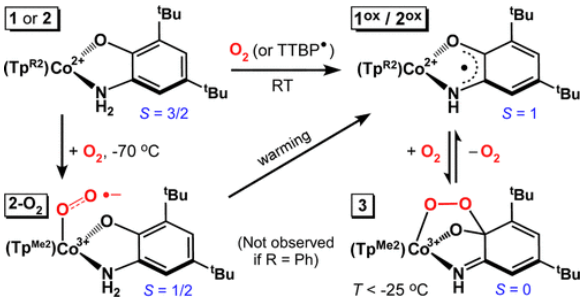

Scheme 2. Species Generated by Reaction of Complexes **1** and **2** with O_2

The “spiroendoperoxide” structure of **3** is the first of its kind among first-row transition metal complexes; indeed, it represents the only X-ray structure to date of a synthetic dioxygen adduct with direct relevance to ring-cleaving dioxygenases. The closest analogues are Rh(III)- and Ir(III)-alkylperoxo complexes generated by O_2 addition to a 9,10-phenanthrene-catecholate(2-) ligand.(13) Similarly, Gade recently reported a square-planar nickel(II) complex that features an alkylperoxometallocycle derived from O_2.(14) In main-group chemistry, Abakumov showed that a series of Sb(V)-amidophenolate complexes reversibly bind O_2 to yield an alkylperoxo donor.(15) As for biological precedents, the structure **3** closely resembles the iron-alkylperoxo intermediate observed by Lipscomb in a crystal structure of HPCD.(16)

As summarized in Scheme 2, we have explored the O_2 reaction landscape of two cobalt(II)-aminophenolate complexes. These studies led to the isolation and characterization of cobalt(III)-superoxo (**2-O_2**) and -alkylperoxo (**3**) species that mimic proposed intermediates of ring-cleaving dioxygenases. It is instructive that subtle differences between these synthetic Co/O_2 adducts and their enzymatic counterparts account for the lack of ring-cleavage activity exhibited by our synthetic models. Specifically, the low-spin Co(III) center of **3** stabilizes the alkylperoxo ligand and prevents subsequent O–O bond cleavage, whereas the high-spin Co(II) ion in the putative enzymatic intermediate facilitates insertion of the distal O atom into the ring via Criegee rearrangement. In our models, the inability of **2-O_2** to convert to the requisite cobalt(II)-alkylperoxo intermediate is likely due to the lack of unpaired spin density within the [Co^{3+}-^{tBu2}APH] unit, which hinders O–C bond formation. The enzyme avoids this scenario by coupling O_2 binding to a proton transfer from the substrate to a conserved second-sphere His residue. According to computational studies, this process yields a superoxo-Co(II)-substrate radical species (**B** in Scheme 1) that is primed for alkylperoxo formation.(17) Future efforts in our laboratory will be directed toward the design of functional active-site mimics that replicate the ability of the enzyme to control both H^+ transfer and O_2 binding.

Supporting Information

The Supporting Information is available free of charge on the ACS Publications website at DOI: 10.1021/jacs.9b05320.

Experimental procedures, computational methods and models, spectroscopic data (EPR, ^{1}H NMR, UV–vis) (PDF)

Crystallographic information (CIF)

pdf

ja9b05320_si_001.pdf (3.9 MB)

crystallographic information file

ja9b05320_si_002.cif (5.58 MB)

The authors declare no competing financial interest.

Terms & Conditions

Acknowledgments

This research received financial support from the National Institutes of Health (GM126522). Improvements to the X-band EPR instrument at Marquette University were funded through a grant from the National Science Foundation (CHE-1532168). We thank Dr. Sheng Cai for assistance with the variable-temperature NMR experiments.

References

1 Wang, Y.; Li, J.; Liu, A. Oxygen activation by mononuclear nonheme iron dioxygenases involved in the degradation of aromatics. *JBIC, J. Biol. Inorg. Chem.* **2017**, *22*, 395– 405, DOI: 10.1007/s00775-017-1436-5

2 Vaillancourt, F. H.; Bolin, J. T.; Eltis, L. D. The ins and outs of ring-cleaving dioxygenases. *Crit. Rev. Biochem. Mol. Biol.* **2006**, *41*, 241– 267, DOI: 10.1080/10409230600817422

3 (a) Koehntop, K. D.; Emerson, J. P.; Que, L. The 2-His-1-carboxylate facial triad: a versatile platform for dioxygen activation by mononuclear non-heme iron(II) enzymes. *JBIC, J. Biol. Inorg. Chem.* **2005**, *10*, 87– 93, DOI: 10.1007/s00775-005-0624-x. (b) Bruijnincx, P. C. A.; van Koten, G.; Klein Gebbink, R. J. M. Mononuclear non-heme iron enzymes with the 2-His-1-carboxylate facial triad: recent developments in enzymology and modeling studies. *Chem. Soc. Rev.* **2008**, *37*, 2716– 2744, DOI: 10.1039/b707179p

4 (a) Emerson, J. P.; Kovaleva, E. G.; Farquhar, E. R.; Lipscomb, J. D.; Que, L. Swapping metals in Fe- and Mn-dependent dioxygenases: Evidence for oxygen activation without a change in metal redox state. *Proc. Natl. Acad. Sci. U. S. A.* **2008**, *105*, 7347– 7352, DOI: 10.1073/pnas.0711179105. (b) Fielding, A. J.; Kovaleva, E. G.; Farquhar, E. R.; Lipscomb, J. D.; Que, L., Jr. A hyperactive cobalt-substituted extradiol-cleaving catechol dioxygenase. *JBIC, J. Biol. Inorg. Chem.* **2011**, *16*, 341– 355, DOI: 10.1007/s00775-010-0732-0. (c) Fielding, A. J.; Lipscomb, J. D.; Que, L. Characterization of an O_2 adduct of an active cobalt-substituted extradiol-cleaving catechol dioxygenase. *J. Am. Chem. Soc.* **2012**, *134*, 796– 799, DOI: 10.1021/ja2095365. (d) Fiedler, A. T.; Fischer, A. A. Oxygen activation by mononuclear Mn, Co, and Ni centers in biology and synthetic complexes. *JBIC, J. Biol. Inorg. Chem.* **2017**, *22*, 407– 424, DOI: 10.1007/s00775-016-1402-7

5 Fielding, A. J.; Lipscomb, J. D.; Que, L., Jr. A two-electron-shell game: intermediates of the extradiol-cleaving catechol dioxygenases. *JBIC, J. Biol. Inorg. Chem.* **2014**, *19*, 491– 504, DOI: 10.1007/s00775-014-1122-9

6 (a) Lipscomb, J. D. Mechanism of extradiol aromatic ring-cleaving dioxygenases. *Curr. Opin. Struct. Biol.* **2008**, *18*, 644– 649, DOI: 10.1016/j.sbi.2008.11.001. (b) Kovaleva, E. G.; Lipscomb, J. D. Versatility of biological non-heme Fe(II) centers in oxygen activation reactions. *Nat. Chem. Biol.* **2008**, *4*, 186– 193, DOI: 10.1038/nchembio.71

7 (a) Dong, G.; Lu, J.; Lai, W. Insights into the Mechanism of Aromatic Ring Cleavage of Noncatecholic Compound 2-Aminophenol by Aminophenol Dioxygenase: A Quantum Mechanics/Molecular Mechanics Study. *ACS*

Catal. **2016**, *6*, 3796– 3803, DOI: 10.1021/acscatal.6b00372. (b) Machonkin, T. E.; Doerner, A. E. Substrate Specificity of Sphingobium chlorophenolicum 2,6-Dichlorohydroquinone 1,2-Dioxygenase. *Biochemistry* **2011**, *50*, 8899– 8913, DOI: 10.1021/bi200855m

8 (a) Wang, P.; Yap, G. P. A.; Riordan, C. G. Five-coordinate M^{II}-semiquinonate (M = Fe, Mn, Co) complexes: reactivity models of the catechol dioxygenases. *Chem. Commun.* **2014**, *50*, 5871– 5873, DOI: 10.1039/C3CC49143A. (b) Wang, P.; Yap, G. P. A.; Riordan, C. G. Synthesis, characterization and O_2 reactivity of a bioinspired cobalt(II)-catecholate complex. *Inorg. Chim. Acta* **2019**, *488*, 49– 55, DOI: 10.1016/j.ica.2019.01.007

9 (a) Agake, S.-i.; Komatsuzaki, H.; Satoh, M.; Agou, T.; Tanaka, Y.; Akita, M.; Nakazawa, J.; Hikichi, S. A monomeric manganese(II) catecholato complex: Synthesis, crystal structure, and reactivity toward molecular oxygen. *Inorg. Chim. Acta* **2019**, *484*, 424– 429, DOI: 10.1016/j.ica.2018.09.013. (b) Ikeda, A.; Hoshino, K.; Komatsuzaki, H.; Satoh, M.; Nakazawa, J.; Hikichi, S. O_2 activation and external substrate oxidation capability of a Co(II)-semiquinonato complex. *New J. Chem.* **2013**, *37*, 2377– 2383, DOI: 10.1039/c3nj00215b

10 Brown, S. N. Metrical Oxidation States of 2-Amidophenoxide and Catecholate Ligands: Structural Signatures of Metal-Ligand pi Bonding in Potentially Noninnocent Ligands. *Inorg. Chem.* **2012**, *51*, 1251– 1260, DOI: 10.1021/ic202764j

11 Bittner, M. M.; Kraus, D.; Lindeman, S. V.; Popescu, C. V.; Fiedler, A. T. Synthetic, Spectroscopic, and DFT Studies of Iron Complexes with Iminobenzo(semi)quinone Ligands: Implications for o-Aminophenol Dioxygenases. *Chem. - Eur. J.* **2013**, *19*, 9686– 9698, DOI: 10.1002/chem.201300520

12 (a) Wang, C.-C.; Chang, H.-C.; Lai, Y.-C.; Fang, H.; Li, C.-C.; Hsu, H.-K.; Li, Z.-Y.; Lin, T.-S.; Kuo, T.-S.; Neese, F.; Ye, S.; Chiang, Y.-W.; Tsai, M.-L.; Liaw, W.-F.; Lee, W.-Z. A Structurally Characterized Nonheme Cobalt-Hydroperoxo Complex Derived from Its Superoxo Intermediate via Hydrogen Atom Abstraction. *J. Am. Chem. Soc.* **2016**, *138*, 14186– 14189, DOI: 10.1021/jacs.6b08642. (b) Oddon, F.; Chiba, Y.; Nakazawa, J.; Ohta, T.; Ogura, T.; Hikichi, S. Characterization of Mononuclear Non-heme Iron(III)-Superoxo Complex with a Five-Azole Ligand Set. *Angew. Chem., Int. Ed.* **2015**, *54*, 7336– 7339, DOI: 10.1002/anie.20150236. (c) Corona, T.; Padamati, S. K.; Acuna-Pares, F.; Duboc, C.; Browne, W. R.; Company, A. Trapping of superoxido cobalt and peroxido dicobalt species formed reversibly from Co^{II} and O_2. *Chem. Commun.* **2017**, *53*, 11782– 11785, DOI: 10.1039/C7CC05904C. (d) Gordon, J. B.; Vilbert, A. C.; Siegler, M. A.; Lancaster, K. M.; Moenne-Loccoz, P.; Goldberg, D. P. A Nonheme Thiolate-Ligated Cobalt Superoxo Complex: Synthesis and Spectroscopic Characterization, Computational Studies, and Hydrogen Atom Abstraction Reactivity. *J. Am. Chem. Soc.* **2019**, *141*, 3641– 3653, DOI: 10.1021/jacs.8b13134. (e) Fischer, A. A.; Lindeman, S. V.; Fiedler, A. T. Spectroscopic and computational studies of reversible O_2 binding by a cobalt complex of relevance to cysteine dioxygenase. *Dalton Trans* **2017**, *46*, 13229– 13241, DOI: 10.1039/C7DT01600J. (f) Jones, R. D.; Summerville, D. A.; Basolo, F. Synthetic oxygen carriers related to biological systems. *Chem. Rev.* **1979**, *79*, 139– 79, DOI: 10.1021/cr60318a002

13 (a) Barbaro, P.; Bianchini, C.; Mealli, C.; Meli, A. Synthetic models for catechol 1,2-dioxygenases. Interception of a metal catecholate-dioxygen adduct. *J. Am. Chem. Soc.* **1991**, *113*, 3181– 3, DOI: 10.1021/ja00008a062. (b) Dutta, S.; Peng, S.-M.; Bhattacharya, S. Ligand Control on Molecular Oxygen Activation by Rhodium Quinone Complexes. *Inorg. Chem.* **2000**, *39*, 2231– 2234, DOI: 10.1021/ic990999v

14 Rettenmeier, C. A.; Wadepohl, H.; Gade, L. H. Structural Characterization of a Hydroperoxo Nickel Complex and Its Autoxidation: Mechanism of Interconversion between Peroxo, Superoxo, and Hydroperoxo Species. *Angew. Chem., Int. Ed.* **2015**, *54*, 4880– 4884, DOI: 10.1002/anie.201500141

15 Abakumov, G. A.; Poddel'sky, A. I.; Grunova, E. V.; Cherkasov, V. K.; Fukin, G. K.; Kurskii, Y. A.; Abakumova, L. G. Reversible binding of dioxygen by a non-transition-metal complex. *Angew. Chem., Int. Ed.* **2005**, *44*, 2767– 2771, DOI: 10.1002/anie.200462503

16 Kovaleva, E. G.; Lipscomb, J. D. Crystal structures of Fe^{2+} dioxygenase superoxo, alkylperoxo, and bound product intermediates. *Science* **2007**, *316*, 453– 457, DOI: 10.1126/science.1134697

17 Cao, L.; Dong, G.; Lai, W. Reaction Mechanism of Cobalt-Substituted Homoprotocatechuate 2,3-Dioxygenase: A QM/MM Study. *J. Phys. Chem. B* **2015**, *119*, 4608– 4616, DOI: 10.1021/acs.jpcb.5b00613